



The Small-Scale Flow Field Around *Dipsastraea favus* Corals

Uri Shavit^{1*}, Tali Mass² and Amatzia Genin³

¹ Civil and Environmental Engineering, Technion, Haifa, Israel, ² Marine Biology Department, The Leon H. Charney School of Marine Sciences, University of Haifa, Haifa, Israel, ³ The Hebrew University of Jerusalem and The Interuniversity Institute for Marine Sciences, Eilat, Israel

Key biological processes that are related to feeding, growth, and mortality in corals and other benthic organisms, depend on the flow field around them. For example, in the absence of flow, oxygen is accumulated inside and around photoautotrophic organisms such as algae and corals, and the rate of photosynthesis is therefore reduced. When mixing by turbulence and by streamline separation is suppressed, nutrient supply is reduced and prey capture becomes insufficient. Despite the overwhelming ecological impacts of flow on corals, almost no *in-situ* studies focused on the hydrodynamics at the scale of the coral polyps and their tentacles. Here we report on *in-situ* measurements obtained by an underwater Particle Image Velocimetry (PIV) above the tentacles of the massive coral *Dipsastraea favus*. The tentacles in this species, approximately 5-10 mm long, extend during the night and contract during the day. A comparison was made between the flow field around the coral when the tentacles were contracted and extended. As in large-scale canopy flows such as forests or urban areas, we found that when the tentacles were extended, a mixing layer rather than a boundary layer was formed above the coral. Velocities in between the tentacles were reduced, resident time increased, and velocity instabilities developed around the tentacle tips. Our *in-situ* measurements under the conditions of contracted tentacles agreed well with laboratory measurements obtained above dead skeletons of *D. favus*. When the tentacles were extended, a velocity profile typical for canopy flows developed, having a clear inflection point near the interface between the tentacles and the layer of free flow. The relative velocity fluctuations increased up to 3.5-fold compared with the state of contracted tentacles. The highest mixing was around the distal ends of the tentacles, where knob-like spheres named acrospheres contain extremely high concentrations of nematocytes. The intense mixing, the ensuing slowing down of prey movement, and its longer residence time within that zone may augment prey capture by the coral. These findings can explain the ubiquitous occurrence of acrospheres in benthic cnidarians.

Keywords: coral tentacles, canopy flow, mixing, mass transfer, particle image velocimetry, *in-situ*, stinging cells

OPEN ACCESS

Edited by:

Anne Staples,
Virginia Tech, United States

Reviewed by:

Gregory N. Nishihara,
Nagasaki University, Japan
Susana Enriquez,
National Autonomous University of
Mexico, Mexico

*Correspondence:

Uri Shavit
aguri@technion.ac.il

Specialty section:

This article was submitted to
Marine Ecosystem Ecology,
a section of the journal
Frontiers in Marine Science

Received: 18 January 2022

Accepted: 11 April 2022

Published: 23 May 2022

Citation:

Shavit U, Mass T and Genin A (2022)
The Small-Scale Flow Field Around
Dipsastraea favus Corals.
Front. Mar. Sci. 9:857109.
doi: 10.3389/fmars.2022.857109

INTRODUCTION

Sessile animals such as corals depend on the flow of water to sustain many of their biological processes (Kaandorp et al., 1996; Finelli et al., 2006; Mass et al., 2010; Goldberg, 2018; Davis et al., 2021). Water flow determines the supply of metabolites from the adjacent water (Patterson and Sebens, 1989; Patterson, 1992; Thomas and Atkinson, 1997), delivers food particles (Sebens et al., 1998), and carries nutrients that eventually cross the coral tissue by diffusion (Sheppard et al., 2018). Flow controls the supply of CO₂ and the removal of oxygen excess to allow photosynthesis (Mass et al., 2010), it influences the rate of heat transfer (Jimenez et al., 2011 and van Woesik et al., 2012) and plays a role in the dispersion and settlement of larvae (Reidenbach et al., 2021). It was suggested that flow, and therefore the rate of mass transfer, change the ability of microbes to settle on coral surfaces and thereby altering the competition between corals and other benthic organisms (Barott and Rohwer, 2012). It is apparent that there is almost no single function that is not affected by the flow of water, including respiration (Nakamura et al., 2005), reproduction (Patterson, 1992), calcification (Dennison and Barnes, 1988), growth (Jokiel, 1978; Mass et al., 2011), and morphological adaptation (Gardella and Edmunds, 2001; Todd, 2008; Mass et al., 2011).

The flow-animal interaction is a multiscale process that depends on the time and length scales of the flow and on the scales of the animals and their surroundings. These latter scales are geometrical in nature and include, among others, the shape of the coastline, the local bathymetry, obstacles that alter the flow in the upstream, and the detailed geometry of the coral reef, coral colonies, coral branches, and their fine roughness elements (Johnson and Sebens, 1993). In a series of review papers, Monismith (2007), Lowe and Falter (2015), and Davis et al. (2021) summarize the current knowledge about the role of flow and its forcing on coral reefs. The three reviews share the understanding that the impact of flow is a result of scale's superposition of regional circulation, mesoscale currents, water movement due to tide, upwelling and internal waves, the velocity field generated by surface waves, and the turbulent scales. Starting from far away, each of these flows carries the metabolites along different distances, from the large ocean far away from the reef, down to the coral tissue finest scales. Each stage in the transport chain is important and any missing stage might prevent the metabolites from reaching the coral. Advection carries solutes and particles along the main flow direction while other processes, such as turbulent mixing, wake flows, and gravity are needed to cross streamlines and move perpendicular to the main currents (e.g., Reidenbach et al., 2021). The interplay between the advection and the lateral mixing occurs at different scales. For example, large turbulent structures that are generated in the flow above the reef penetrate the reef through its top interface. Smaller turbulent structures are generated by the flow interaction with the coral colonies and branches and penetrate the top interface of each colony. And finally, local roughness elements along individual coral branches augment mixing and lateral fluxes. This complex

geometry, including the height of the roughness elements and the distance between them, controls the mixing intensity as address by previous studies (Stocking et al., 2018 and Davis et al., 2021). Studies that focused on coral hydrodynamics analyzed the role of reef scales (Hench et al., 2008; Lowe et al., 2009), colony scales (Rosman and Hench, 2011), and branch scales (Asher et al., 2016 and Asher and Shavit, 2019), but only a few studied the role of smaller scales (Shapiro et al., 2014). The analysis is crucial for mass transfer estimates at these large scales but might miss the governing mechanisms that occur at smaller scales. For example, depth-integrated transport equation, commonly used to analyze mass transfer inside coral reefs (e.g., Falter et al., 2008), cannot distinguish between processes that occur at different heights within the reef. The same is with studies that treat the coral colonies and coral branches as roughness elements (Hench and Rosman, 2013). They provide quantitative estimates for the mixing between the ambient water and the space between the colonies but ignore the stage of mass transfer from the water between the colonies and between the coral branches to the actual living tissue.

Most stony corals are modular animals, forming colonies of numerous polyps that are connected by a common gastrovascular system. The polyps, ranging in size from sub-millimeter to a few centimeters, are fleshy and flexible. The polyps themselves, like miniature anemones, have tentacles that capture zooplankton by hydrodynamics-dependent, filter-feeding mechanisms (Patterson, 1991; Sebens and Johnson, 1991). Coral tentacles demonstrate different extension/contraction patterns. In most species, especially those with large polyps (Levy et al., 2006), the tentacles are extended only during the night. In some species, all with minute polyps, the tentacles are always extended, while in some rare species the expansion is only during the day (Eguchi, 1936; Abe, 1939; Kawaguti, 1954; Porter, 1974; Lewis and Price, 1975; Sweeney, 1976; Levy et al., 2001; Levy et al., 2006).

Coral tentacles are used for prey capturing, as a defense tool against predators, and when competing on territory against other corals. Levy et al. (2001) reports that tentacles that extend during the day are rich in symbiotic algae and postulate that they extend to increase photosynthesis. However, the large number of corals that contract during the day suggests that photosynthesis does not serve as the prime reason for extension. Zooplankton, on the other hand, is more abundant at night (Sorokin, 1990), suggesting that the reason most corals extend at night is prey capture. Shashar et al. (1993) and Levy et al. (2001) also found that tentacles expansion increases with water velocity and proposed that respiration gains from the increase in surface area. According to Levy et al. (2003), extended tentacles increase the tissue surface area of the *Goniopora lobata* by ~8 fold compared to the contracted tentacles state. Such an area increase allows higher uptake when the tentacles are extended. Many corals use their tentacles to host numerous stinging cells (nematocytes), used mostly for prey capture (Sheppard et al., 2018). These nematocytes are often distributed as clusters along the tentacle and in a knob-like sphere, called acrosphere, positioned at the tentacle tip. The acrospheres contain an extremely high concentration of stinging cells (Acuña and

Garese, 2009). By adopting the description of mass transfer as a chain of stages, solutes and particles that reach the space near the corals need extra means to be mixed and approach the coral tissue, the tentacles, and their nematocytes.

In the current study we focus on the role of coral tentacles as a mean to increase lateral mixing. We will show that the tentacles impose hydrodynamic mixing and therefore support the lateral motion towards the coral tissue. We present *in-situ* velocity measurements of the flow above two stony *D. favus* corals under a wide variety of natural conditions and compare the flow field when the tentacles are contracted and when they are extended (Figures 1, 2).

METHODS

Measurement Site and the *Dipsastraea favus* Corals

In-situ velocity measurements were taken above two *Dipsastraea favus* colonies, a stony species commonly found in the northern parts of the Gulf of Aqaba (Red Sea). It is the dominant species on the reef back margins. Colonies are massive, rounded, or flat with large polyps (average polyps' diameter is more than 12 mm) and long tentacles (the average tentacles length in the current study was ~ 0.6 cm, Table 1) (Figure 1). We found that the length of the extended tentacles, ℓ , was longer (6–8 mm) in Coral I and shorter (4–5 mm) in Coral II (Table 1). The colonies length (in the dominant flow direction), width, and height were $L = 120$, $W = 115$, and $H = 65$ mm in the first colony (Coral I) and $L = 100$, $W = 80$, and $H = 60$ mm in the second (Coral II). The velocity measurements were collected at a depth of f 4–5 m in the reef adjacent to the Interuniversity Institute for Marine Sciences (IUI), Eilat, Israel (29°30'N, 34°55'E). They were collected at night when the coral tentacles are naturally extended. Tentacle's contraction (Figure 2A) was achieved by scuba divers that gently touched the corals. Once contracted, it took 20–30 minutes for the tentacles to re-extend (Figure 2B), giving us enough time to measure the velocity field around the contracted coral and enough contraction/extension cycles during a measurement night.

Underwater Particle Image Velocimeter (UPIV)

A self-design Underwater Particle Image Velocimeter (UPIV) was constructed and deployed for *in-situ* velocity measurements. The system consists of two 200 mJ per pulse Nd: YAG lasers (Quantel), a 12-bit 1024 × 1392 pixels dual shutter CCD camera (PCO, Pixelfly qe), and a 200 mm Nikkor lens. Both the lasers and camera were set to operate at 5 frames per second. The lasers and camera were installed inside waterproof housings that were manufactured in-house and mounted on a stable metal frame (1.85 m long, 1.5 m wide and 1.6–2.0 m flexible height) positioned on the seafloor (Figure 2C). The freedom to change the frame height was achieved by using four adjustable scaffolding legs, allowing fine adjustment of their height while underwater. Fine adjustment of the housings lateral position was achieved by homemade linear translation screws that were fixed to the frame. The system's control station was positioned on the IUI pier. It was connected to the underwater lasers and camera through three 15 m long waterproof umbilical hoses. Two hoses were connected to the lasers housing and used to deliver water for laser cooling and electrical wires for laser triggering, power supply, heat dissipation by an internal fan, and monitoring the housing inner temperature and relative humidity (read by sensors that were installed inside the housing). The third umbilical hose was connected to the camera housing to provide power supply, triggering, and image acquisition (using StreamPix software, Norpix). Before deployment and before sealing the housings, the laser light sheet (532 nm wavelength and ~ 1 mm thick) was aligned and its intensity was optimized. Simultaneously, the camera iris and focus were adjusted using a large glass container filled with seawater that was positioned on the pier under the laser.

The assembled sealed system was deployed from the pier using a crane and then positioned and anchored to the sea bottom by scuba divers. The scuba divers focused the laser beam and the camera image using the linear translation screws. They positioned the vertical laser light sheet above the coral center, and together with the team on the pier, performed a calibration procedure by capturing images of a vertical ruler, positioned

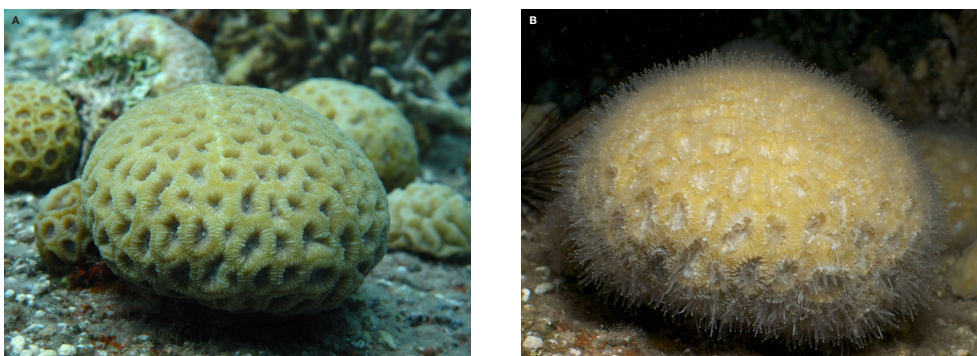
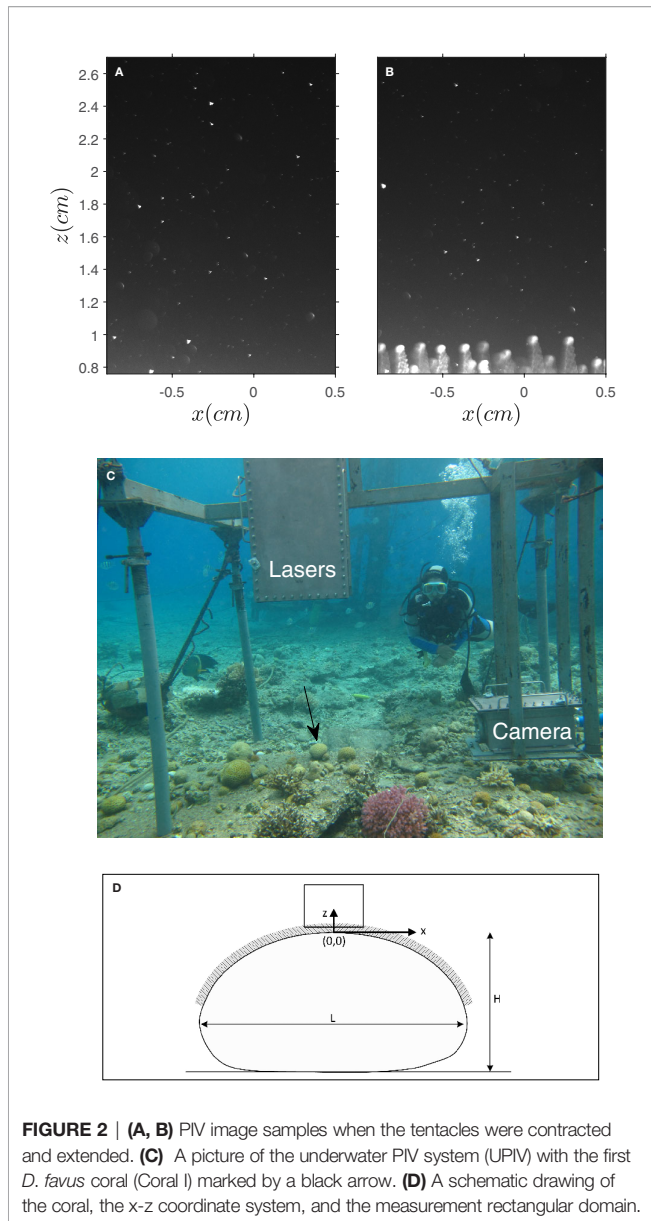


FIGURE 1 | Pictures of the *D. favus* coral during the day when its tentacles are contracted (A) and during the night when the tentacles are extended (B).



such that $z = 0$ was set at the top of the coral when contracted (**Figure 2D**). Communication between the underwater and pier teams was made possible by an underwater monitor, which mirrored the camera vision and allowed the pier team to send text instructions to the divers. The measurements were typically collected from sunset to sunrise, as dark conditions provide a black background and high contrast needed for the PIV grayscale images. Working at night also helps to prevent casual swimmers from approaching the measurement area, maintaining high operational safety.

We noticed that following a few hundred laser pulses, the coral tentacles started to contract. In some cases, the length of the tentacles became shorter and in others the coral contracted its tentacles all the way to a full contraction. After such a contraction, we turned the laser off and paused for 10-20 minutes before the

tentacles were extended again and measurements could be resumed. The number of collected image pairs when the tentacles were extended or contracted is reported in **Table 1**. Since the ambient velocity varied between measurements, the time delay between the first and second PIV images was continuously adjusted, providing a particle shift of ~ 10 pixels.

Velocity vectors were calculated using a modified version of the MatPIV open-source code (Sveen, 2004). Image magnification was $52.7 \text{ pixels mm}^{-1}$ in Coral I and $47.1 \text{ pixels mm}^{-1}$ in Coral II, yielding a field of view of about $25 \times 20 \text{ mm}^2$. In some cases, light reflection occurred when the elongated tentacles appeared at the bottom of the images. The reflection was more severe during the measurements above Coral II than above Coral I. Even without reflection, the white color of the tentacles often reduced the quality of the PIV results. To eliminate this effect, we masked out these white regions (typically 2-4 lines of vectors out of 29 horizontal lines) and analyzed only the non-masked regions. Naturally occurring particles were used as tracers and therefore, prior to the PIV processing, intensity capping (Shavit et al., 2007) was applied to reduce the noise due to large particles that do not follow the water flow. A multi-pass cross-correlation was applied using square interrogation areas of 128×128 , 128×128 , 64×64 and 64×64 pixels. At the current magnification, a smaller interrogation area could not be used because of the small density number of the natural particles. An overlap of 50% results in a distance between neighboring velocity vectors of 32 pixels, equivalent to $0.6 - 0.68 \text{ mm}$. Outliers were identified by a detailed examination of a signal-to-noise ratio filter followed by a global filter and a local filter. When rejected, the empty vector was filled by a kernel-based interpolation linear scheme, based on 3×3 and 5×5 neighbor vectors. The threshold values of the signal-to-noise ratio, standard deviation of the global filter, and that of the local filter were 1.05-1.1, 2.5-4.0, and 2.2-3.2, respectively, rejecting an average of 10.8% of the velocity vectors.

Spectral analyses of the velocity time series have shown that the time and length scales of the wave and turbulent components often overlap. We therefore decompose the instantaneous velocity u_i as,

$$u_i = u_i^c + u_i^{wt} \quad (1)$$

where u_i^c is the current velocity and u_i^{wt} is the sum of the wave contribution u_i^w and the turbulent contribution u_i^t ($u_i^{wt} = u_i^w + u_i^t$). The index i is used to represent the velocity components, u and w in the x and z directions. We found that while the separation of u_i^{wt} into the wave and turbulent contributions involves some ambiguities, the current component is well distinct and can be separated by a low-pass filter for frequencies below 0.03 Hz . In a few cases, a clear separation was possible between the wave and turbulent fluctuations for which u_i^w and u_i^t were computed (see **Supplementary Material**).

Laboratory PIV

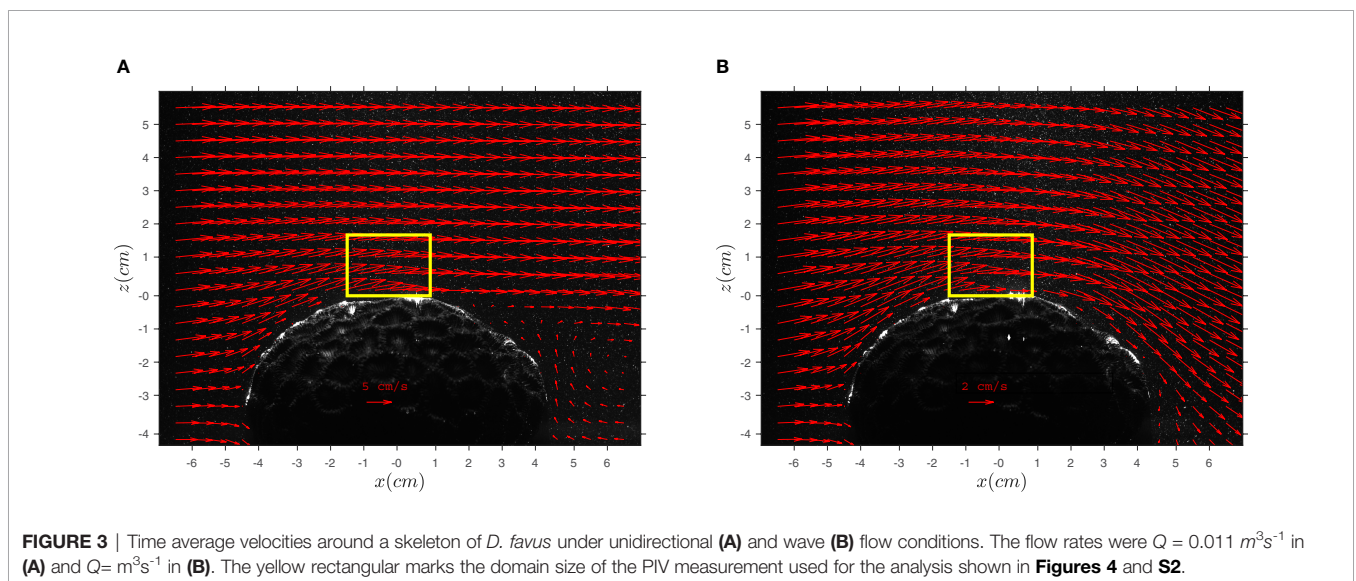
Velocity measurements were obtained in a laboratory hydraulic flume around a *D. favus* skeleton ($L = 87$, $W = 81$, and $H \cong 50 \text{ mm}$) under steady unidirectional and wave flow conditions (at a

TABLE 1 | Experimental conditions including the spatial and temporal mean (in space and time) velocity in the x direction (positive is north to south), the mean velocity at the top of the measured domain, the root mean square of the wave and turbulent fluctuating velocity, $u^{wt} + u^t$, the number of realization, the tentacle length, the dominant wave frequency, and two Reynolds numbers.

Set #	Mean velocity	Velocity at top	Wave & turb RMS	Number of realizations	Tentacle length	Wave frequency	Reynolds numbers	
	\bar{u} ($cm\ s^{-1}$)	\bar{u}_{top} ($cm\ s^{-1}$)	$(u^{wt}_{RMS})_{top}$ ($cm\ s^{-1}$)	(-)	ℓ (cm)	f (s^{-1})	Re	Re_{δ}
Coral I, Contracted tentacles:								
C1	-3.60	-3.57	2.12	1000		0.42	4302	19
C2	-2.67	-2.63	2.01	1000		0.34	3169	20
C3	4.38	4.43	0.95	500		0.41	5339	8
C4	3.61	3.72	0.87	500		0.29	4483	9
Coral I, Extended tentacles:								
E1	-3.80	-3.93	5.63	250	0.6	0.26	4736	63
E2	1.65	1.80	3.92	500	0.65	0.28	2169	42
E3	1.27	1.47	4.27	250	0.7	0.32	1772	43
E4	-1.83	-1.96	4.25	500	0.8	0.31	2362	44
E5	-2.74	-2.78	3.78	500	0.8	0.25	3350	43
Coral II, Contracted tentacles:								
C11	8.06	7.97	1.47	1000		0.37	7357	14
C12	8.95	9.03	2.71	1000		0.47	8335	23
C13	11.8	11.8	3.11	1000		0.41	10892	28
C14	8.48	8.62	2.61	1000		0.43	7957	23
Coral II, Extended tentacles:								
E11	9.34	9.74	1.33	200	0.5	0.37	8991	12
E12	6.71	7.03	1.96	500	0.45	0.45	6489	17
E13	6.23	6.48	2.00	500	0.45	0.44	5982	17
E14	11.4	12.1	3.75	500	0.5	0.40	11169	34
E15	-5.61	-5.61	0.94	1000	0.4		5178	
Skeleton								
S1	3.41	3.85	0.49	1000			1703	
S2	9.69	10.1	0.72	1000			4845	

wave frequency of 0.5 Hz). The experimental setup, including the flume, flow rate measurements, and the laboratory PIV are described in Moltchanov et al. (2015). Since the ambient velocities during the *in-situ* measurements around coral II were higher than during the coral I measurements, a high and low flow rates were tested in the laboratory ($Q = 0.0036\ m^3\ s^{-1}$ and $Q =$

$0.011\ m^3\ s^{-1}$). In addition to the 200 mm Nikkor lens that was used also in-situ, a 50 mm lens (Goyo Optical Inc.) was used to illustrate the flow around the whole colony (Figure 3). For the wave flow case, we superimposed surface waves on a steady flow rate of $Q = 0.0036\ m^3\ s^{-1}$ using a paddle wave generator that was positioned near the flume inlet. Figure 3 shows the time average velocity field



under unidirectional flow (Figure 3A) and wave flow conditions (Figure 3B). Notice the different flow conditions in the wake region of the unidirectional and wave flow conditions (see for example Figure 2 in Yu et al., 2022).

Experimental Conditions

In situ measurements were obtained above two corals (coral I and coral II) under extended (E) and contracted (C) tentacle conditions, a total of four measurement groups. Table 1 lists the experimental conditions of these four groups. It includes the mean velocity (\bar{u}), obtained by averaging the velocity x -component over time and space within the whole measured field, the mean velocity at the top of the domain (\bar{u}_{top}), obtained by averaging the temporal mean along the x coordinate (the flow direction) at the highest measured location of the flow field, the root mean square of the turbulent + wave velocity fluctuations at the top of the domain [$(u_{RMS}^{wt})_{top}$], the number of realizations in each group (at 5 Hz), the average length of the tentacles (ℓ) observed during the experiments, and the wave dominant frequency (f). Two Reynolds numbers were chosen to represent the flow; $Re = \bar{u}_{top}H/\nu$ where H is the coral height and $\nu = 9.75 \cdot 10^{-3} \text{ cm}^2\text{s}^{-1}$ is the kinematic viscosity of seawater at 24.5°C representing the mean flow around the coral colony, and $R_\delta = (u_{RMS}^{wt})_{top} \delta/\nu$ with $\delta = \sqrt{2\nu/\omega}$ as a measure of the thickness of the viscous bottom boundary layer (Mazzuoli et al., 2017) where $\omega = 2\pi f$ is the angular frequency of the velocity oscillations. A comparison between the two corals shows that while coral II is smaller and has shorter tentacles than in coral I, most of the mean velocities were higher when measured around coral II. The overall larger Re around coral II reflects the higher velocity more than the coral size. The results obtained for R_δ serve as an indication of the waves and velocity fluctuations above the corals. The table shows that R_δ of coral II is similar in both contracted and extended cases, however R_δ of coral I is low when the tentacles were contracted and high when the tentacles were extended.

RESULTS AND DISCUSSION

Levy et al. (2001) reports that *Dipsastraea favus* corals do not extend their tentacles in still water even if light is low and prey levels are high enough. It suggests that the coral extended tentacles are useful only if the flow conditions are adequate. They also found that if no prey is present, the corals will still extend, but only if light is low and flow speed is medium to high, suggesting that prey capture is probably one of several benefits gain by tentacle extension. Here we show how the flow is modified by the extended tentacles.

The flow of sea water around the *Dipsastraea favus* colonies is influenced by the oblate spheroid shape of the coral (Figure 3). It involves a small region of reduced velocities on the upstream (windward) side of the coral, followed by a region of crowded streamlines and high velocities, a flow region that is roughly parallel to the coral surface, and then, depending on the wave conditions, separation of streamlines and recirculation in the wake side of the colony. Each of these flow regions experiences different flow conditions and different mass transfer processes, however they share the need to transfer commodities across

streamlines. The reported measurements focus on the region at the top of the colony where the flow is approximately parallel to the coral surface (yellow rectangle in Figure 3). In addition to the influence of the coral geometry, the flow near the coral is affected by the action of surface waves, by the extension of the polyps' tentacles, and by their flexibility and potential bending by the flow. Under these complex flow conditions, the *in-situ* study aims at quantification the role of the tentacles extension by comparing the flow near the coral when the tentacles are extended (Figure 2B) and when they are contracted (Figure 2A).

Figure 4 shows the x -component of the mean velocity (temporal averaged) as a function of vertical distance from the coral surface, z (Figure 2D). The mean velocity was averaged along x and then normalized by its' value at the top, \bar{u}_{top} (Table 1). The measurements above both corals (Figures 4A, B) indicate that when the tentacles are contracted (sets C1-C4 and C11-C14), the velocity profiles are nearly uniform. The velocities near the skeleton (Q1 and Q2, both under unidirectional flow) show the influence of the non-slip condition as they were measured close to the surface, suggesting that the velocity profiles resemble a boundary layer with no inflection point. Gardella and Edmunds (2001) measured the shear velocity, u^* , above scleractinian corals and analyzed the boundary layer that develops above the coral as a function of colony size and roughness. Their findings are relevant when the coral tentacles are contracted, however no flow information is available when the tentacles are extended. The results in Figure 4 show that when the tentacles are extended (sets E1-E5 and E11-E15), the relative velocity is reduced (to ~60% in set E3 of coral I and < 10% in set E12 of coral II), developing profiles that resemble a mixing layer rather than a boundary layer. This reduction was observed in all the elongated sets except for two profiles (E1 and E5).

The reduced velocities slow down the food particles. The reshaping of their profiles augment mixing and help the coral polyps to capture them. The rate of mass transfer is expected to be affected by the increase in resident time, the increase of surface area, and the increased mixing intensity. The mixing layer that appears when the tentacles are extended is typical to larger scale canopy flows such as forest canopy (Kaimal and Finnigan, 1994, Chap. 3), urban canopy (Coceal et al., 2006), and flow above branched coral reefs (Davis et al., 2021). Such mixing layers are characterized by an inflection point near the canopy top, that leads to hydrodynamic instabilities such as Kelvin-Helmholtz instabilities (Ghisalberti and Nepf, 2002). As shown, inflection points in sets E2, E3, E11, and E15 are found at $z/\ell = 1.7, 1.8, 0.9$ and 1.1 , respectively. The inflection points indicate that the extension of the tentacles generate a change in the velocity gradient, forming a region of mixing. As expected, the location of the inflection point was found in the sets of coral II around the tip of the extended tentacles, $z/\ell = 1$. In coral I, the inflection location was higher ($z/\ell > 1$), but we assume that it reflects an under estimation of the tentacle length (ℓ). These instabilities are known to be a source of intensive exchange motion of fluid across the canopy interface (Nepf, 2012) and large fluctuations of the measured velocity.

The velocity fluctuations are shown by three representations: the root mean square (RMS) of the velocity

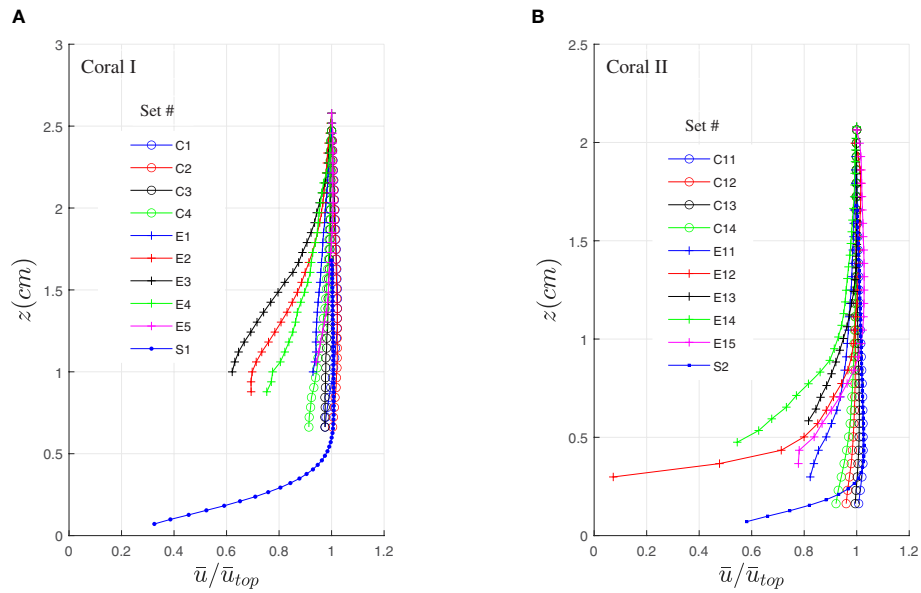


FIGURE 4 | Mean horizontal velocity, \bar{u}/\bar{u}_{top} , above coral I **(A)** and coral II **(B)** versus height above the corals. Measurements were taken when the tentacles were contracted and extended. For comparison, the same measurements were obtained above a skeleton of *D. favius* in the laboratory. C- contracted, E- extended, S-skeleton.

fluctuations, $RMS(u_i - \bar{u}_i) = u_{RMS}$, shown in **Figure S1** (see **Supplementary Material**); the RMS of the sum of the wave and turbulent components, $RMS(u_i^{wt}) = u_{RMS}^{wt}$, shown here in **Figure 5**; and when available, the RMS of the turbulent component, $RMS(u_i^t) = u_{RMS}^t$, shown in **Figure S2**

(Supplementary Material). As u_{RMS} is contaminated by the low frequencies of the ambient flow (u_c) and u_{RMS}^t is ambiguous due to the difficulty to separate the scales of the turbulent signal from the scales of the wave signal, we chose to show here the results of u_{RMS}^{wt} (**Figure 5**) and leave the other two to the

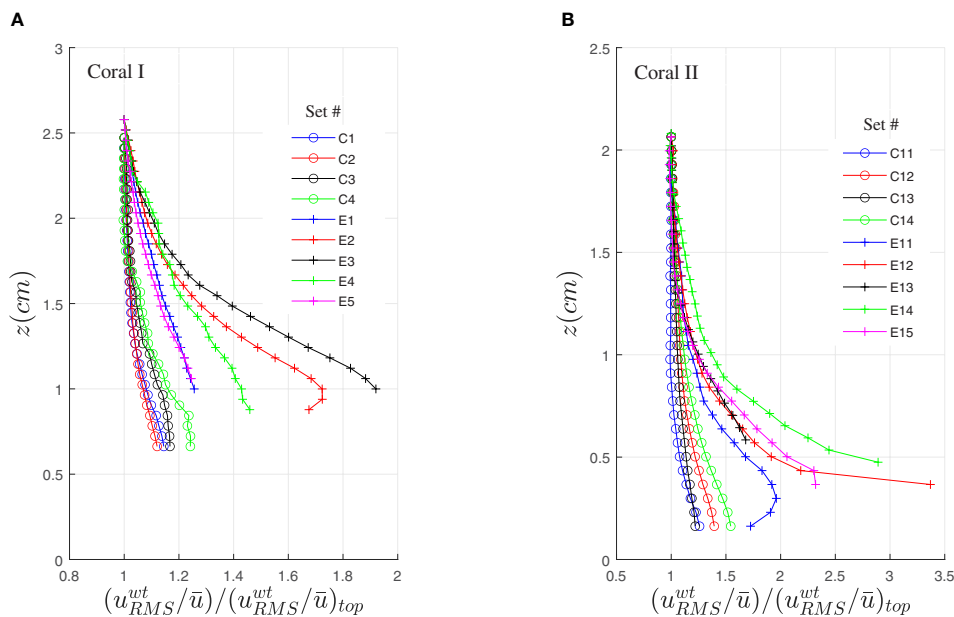


FIGURE 5 | The root mean square of the sum of the turbulent and wave velocity components, divided by the mean velocity, \bar{u} , and normalized by the value at the top of the measured domain. The measurements were obtained when the tentacles were contracted and extended above coral I **(A)** and coral II **(B)**.

Supplementary Material (Figures S1, S2). As in **Figure 4**, u_{RMS}^{wt}/\bar{u} was averaged along x and normalized by the value at the top. **Figure 5** shows that $(u_{RMS}^{wt}/\bar{u})/(u_{RMS}^{wt}/\bar{u})_{top}$ is small in all the contracted cases and high when the tentacles are elongated. The shape of the profiles in the contracted cases is nearly uniform with somewhat higher values near the bottom where shear stress is high. Such profiles characterize boundary layer flows, where the velocity gradient and the velocity fluctuations are the highest when approaching the boundary. However, in the canopy flow generated by the extended tentacles, the highest shear and strongest fluctuations are measured around the tip of the tentacles, at a distance of $z \cong \ell$ from the surface. Moreover, u_{RMS}^{wt} reaches a maximum in sets E2, E11 and potentially in E15 with an excellent agreement with the location where inflection points appeared in the mean velocity profiles (**Figure 4**). The results in **Figure 5** are impressive when considering the large relative increase in u_{RMS}^{wt} relative to $(u_{RMS}^{wt})_{top}$, with a ratio ~ 2 and ~ 3.5 in coral I and coral II, respectively. Such a large increase in fluctuations leads to intensive mixing between the ambient water and the water between the tentacles.

The literature of canopy flows is rich and includes studies of air flow through forests (Finnigan, 2000 and Belcher et al., 2012), air flow through urban areas (Britter and Hanna, 2003, and Ramponi et al., 2015), and water flow through aquatic vegetation and kelp forests (Nepf, 2012 and Rosman et al., 2007), to name a few. The identification of the flow around the coral tentacles as a canopy flow allows us to use the literature to describe the flow between the tentacles, where the access of the PIV was limited. The flow structure inside the canopy is typically classified by two layers; the wake zone (Böhm et al., 2013) and the exchange zone (Ghisalberti and Nepf, 2006). Momentum from the high velocities above the canopy penetrates the exchange zone, generating mixing that drives the flux of momentum, mass, and energy. At around half the canopy height, where most of the momentum was adsorbed by the local drag in the exchange zone, wake turbulence is generated by the local obstacles (the coral tentacles in our case). The mean and turbulent velocities are reduced from their peak at the interface down to zero at the bottom (Moltchanov et al., 2015; Asher et al., 2016). This is the case in flows above forest canopies, aquatic vegetation, and branched coral reefs. We suggest that this is also the case here, between the coral tentacles, where the local velocity field controls the supply of nutrients, the rate of respiration and photosynthesis, and the efficiency of particle capture. Although this mechanistic understanding lays the ground for modeling and prediction of the transport phenomena, it is understood that prediction of the flow between the tentacles of the *D. favus* coral must consider the ellipse shape of the coral, the role of waves (Lowe et al., 2008), the tentacles flexibility (Ghisalberti and Nepf, 2006 and du Roure et al., 2019), and the tentacle's mechanical properties (Koehl, 1999).

Benthic zooplanktivores such as *D. favus* corals capture food particles such as copepods and fish larvae (Sheppard et al., 2018). They capture their prey using stinging cells (nematocysts) that extend their tubules into the water (Park et al., 2017). Although nematocyst's tubules are impressively long compared to the

diameter of their capsules (10 to 100 times), the distance they can reach away from the coral surface is limited (a few tens to a few hundred microns). The number of prey particles in the thin fluid layer that surrounds the coral and can be reached by the nematocyst's tubules is small and is likely to be depleted fast. One of the benefits of the extended long tentacles is an increased surface area (Levy et al., 2006), however, such an advantage is useless if the water contains no prey. As with the supply fluxes that carry nutrients and dissolved gas from the ambient water to the coral surface, the availability of prey particles depends on the ability of hydrodynamic mixing to cross the mean current streamlines and bring the particles close to the coral tissue. Levy et al. (2006) reports that the oxygen consumption of *Favia favus* during the night, when the tentacles are extended, is 20% higher than during the day. The increase in O_2 consumption may serve as proxy of the energy cost of inflating the tentacles by the inner cilia (Levy et al., 2006). The results in **Figure 5** suggest that the benefit of this energetic cost is the intense mixing the tentacles provide. Without this mixing, nutrients and dissolved gas might not have the time to diffuse to the coral surface and prey particles might miss the coral tentacles and the nematocysts reach.

A close examination of the tentacles in **Figure 6** (seen also in **Figures 1B, 2D**) shows that they contain batteries of stinging cells along the tentacles, and in particular, a knob-like structure at the tentacles' tip, called acrosphere. These acrospheres are characterized by a dense layer of nematocytes (Acuña and Garese, 2009; Yosef et al., 2020), exactly where the hydrodynamic mixing is the highest (see set E2 in **Figure 5A** and sets E11 and E15 in **Figure 5B**). One may wonder if the increased number of nematocysts, exactly where mixing intensity is the highest, is adaptive for food capture.

Finally, we note that the mixing mechanism shown in **Figure 5** joins another mass transfer mechanism that we recently found (Malul et al., 2020). It was discovered that coral tentacles move with a phase difference under wave flow conditions. While both the tentacle velocity and the orbital velocity share the frequency of the surface waves, the tentacles periodic motion precedes that of the orbital water velocity, generating higher relative velocities between the water and the tentacle surface, increasing the mass transfer fluxes between the ambient water and the coral. We emphasize, however, that without the canopy mixing reported here, the impact of the phase difference mechanism is limited to the available commodities that have reached the coral vicinity.

CONCLUSIONS

Our *in-situ* measurements suggest that the flow field in and around extended tentacles in *Dipsastraea favus* resembles the hydrodynamic characteristics of a canopy flow. Canopy flows occur above forests, urban areas, and aquatic vegetation, and although they are different in the flowing fluids and length scales, they share many flow characteristics. The canopy region reduces the fluid velocity between the tentacles and increases the retention time. The reduced flow speed is likely to make nutrient uptake more

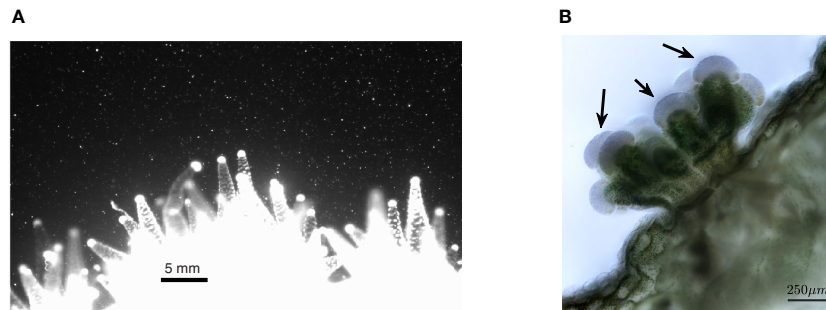


FIGURE 6 | (A) Image of a *D. favus* colony taken in the laboratory. The colony is smaller than the *in-situ* colonies shown in **Figures 1, 2**. Batteries of nematocysts are shown as white spots distributed along the tentacles. The acrospheres are shown as knob-like white spheres at the tip of each tentacle. The nematocyst concentration in these acrospheres is high, resulting in optical saturation. Photo by Dror Malul. **(B)** *In-vivo* light microscopy imaging of *Stylophora pistillata* polyp/tentacle. A dense layer of nematocytes is shown at the acrospheres at the tip of the tentacle (see arrows). The green color is due to the alga symbionts. Photo by Shany Levy.

efficient by increasing the time available for diffusion, and improve prey capturing, as strong flows can induce prey detachment and escape. We showed that the canopy region in a mixing layer rather than a boundary layer, high root-mean-square velocities, and an increase in the relative wave orbital velocity around the tips of the tentacles. The flow at the far tips of the *D. favus* tentacles is a source of instability, equivalent to the upper interface of forest trees and the roofs in a dense urban neighborhood. The interface interactions generate large velocity fluctuations and therefore an intense mixing of mass, momentum, and energy across the interface. While such flows were investigated intensively for flows through forests and aquatic vegetation, no such investigation was obtained for the case of coral tentacles. The idea that the hydrodynamic conditions at that interface increase the probability of prey capture around the tips of tentacles is likely the adaptive reason for the unusually high density of stinging cells at those spots, a characteristic shared by many members of the phylum Cnidaria.

DATA AVAILABILITY STATEMENT

The raw data supporting the conclusions of this article will be made available by the authors, without undue reservation.

AUTHOR CONTRIBUTIONS

All authors designed the study, designed the UPIV system, and carried out the experiments. TM led the UPIV system

REFERENCES

- Abe, N. (1939). On the Expansion and Contraction of the Polyp of a Coral Reef *Caulastrea Furcata* Dana. *Palao. Trop. Biol. Stn. Stud.* 1, 651–670.
- Acuña, F. H., and Garese, A. (2009). The Cnidae of the Acrospheres of the Corallimorpharian *Corynactis Carnea* (Studer 1878) (Cnidaria, Corallimorpharia, Corallimorphidae): Composition, Abundance and Biometry. *Belg. J. Zool.* 139 (1), 50–57.

manufacturing. US undertook the data analysis. All authors contributed to the drafting of the manuscript. All authors read and approved the final manuscript.

FUNDING

This research was supported by the Israel Science Foundation (Grants 620/07 and 1487/10).

ACKNOWLEDGMENTS

We thank the Interuniversity Institute for Marine Sciences (Eilat/Israel) for providing the infrastructure and endless help while constructing and deploying the UPIV system. We thank Yaniv Mass and Yuval Mass for their assistance in the design and manufacturing of the UPIV frame and casings, the scuba divers that assisted during long nights of data collection (Maya Kremien, Oded Ben Shaprut, and Genadi Zalzman), and to Roi Holzman, Stephen Monismith, Dror Malul, and Shai Asher for the discussions about the study topic.

SUPPLEMENTARY MATERIAL

The Supplementary Material for this article can be found online at: <https://www.frontiersin.org/articles/10.3389/fmars.2022.857109/full#supplementary-material>

- Asher, S., Niewerth, S., Koll, K., and Shavit, U. (2016). Vertical Variations of Coral Reef Drag Forces. *J. Geophys. Res. Ocean* 121, 3549–3563. doi: 10.1002/2015JC011428
- Asher, S., and Shavit, U. (2019). The Effect of Water Depth and Internal Geometry on the Turbulent Flow Inside a Coral Reef. *J. Geophys. Res.: Ocean.* 124 (6), 3508–3522. doi: 10.1029/2018JC014331
- Barott, K. L., and Rohwer, F. L. (2012). Unseen Players Shape Benthic Competition on Coral Reefs. *Trends Microbiol.* 20, 621–628. doi: 10.1016/j.tim.2012.08.004

- Belcher, S. E., Harman, I. N., and Finnigan, J. J. (2012). The Wind in the Willows: Flows in Forest Canopies in Complex Terrain. *Annu. Rev. Fluid. Mech.* 44, 479–504. doi: 10.1146/annurev-fluid-120710-101036
- Böhm, M., Finnigan, J. J., Raupach, M. R., and Hughes, D. (2013). Turbulence Structure Within and Above a Canopy of Bluff Elements. *Bound.-Lay. Meteorol.* 146 (3), 393–419. doi: 10.1007/s10546-012-9770-1
- Britter, R. E., and Hanna, S. R. (2003). Flow and Dispersion in Urban Areas. *Annu. Rev. Fluid. Mech.* 35, 469–496. doi: 10.1146/annurev.fluid.35.101101.161147
- Coccal, O., Thomas, T. G., Castro, I. P., and Belcher, S. E. (2006). Mean Flow and Turbulence Statistics Over Groups of Urban-Like Cubical Obstacles. *Bound.-Lay. Meteorol.* 121, 491–519. doi: 10.1007/s10546-006-9076-2
- Davis, K. A., Pawlak, G., and Monismith, S. G. (2021). Turbulence and Coral Reefs. *Annu. Rev. Mar. Sci.* 13, 343–373. doi: 10.1146/annurev-marine-042120-071823
- Dennison, W. C., and Barnes, D. J. (1988). Effect of Water Motion on Coral Photosynthesis and Calcification. *J. Exp. Mar. Biol. Ecol.* 115, 67–77. doi: 10.1016/0022-0981(88)90190-6
- Eguchi, M. (1936). Corals and Coral-Reefs of the Palao Islands Under Japanese Mandate. *Cont. Inst. Geol. Paleont.* 16, 1–49.
- du Roure, O., Lindner, A., Nazockdast, E. N., and Shelley, M. J. (2019). Dynamics of Flexible Fibers in Viscous Flows and Fluids. *Annu. Rev. Fluid. Mech.* 51, 539–572. doi: 10.1146/annurev-fluid-122316-045153
- Falter, J. L., Lowe, R. J., Atkinson, M. J., Monismith, S. G., and Schar, D. W. (2008). Continuous Measurements of Net Production Over a Shallow Reef Community Using a Modified Eulerian Approach. *J. Geophys. Res.* 113, C07035. doi: 10.1029/2007JC004663
- Finelli, C. M., Helmut, B. S. T., Pentcheff, N. D., and Wethey, D. S. (2006). Water Flow Influences Oxygen Transport and Photosynthetic Efficiency in Corals. *Coral. Reef.* 25 (1), 47–57. doi: 10.1007/s00338-005-0055-8
- Finnigan, J. (2000). Turbulence in Plant Canopies. *Annu. Rev. Fluid. Mech.* 32, 519–571. doi: 10.1146/annurev.fluid.32.1.519
- Gardella, D. J., and Edmunds, P. J. (2001). The Effect of Flow and Morphology on Boundary Layers in the Scleractinians *Dichocoenia Stokesii* (Milne-Edwards and Haime) and *Stephanocoenia Michilini* (Milne-Edwards and Haime). *J. Exp. Mar. Biol. Ecol.* 256, 279–289. doi: 10.1016/S0022-0981(00)00326-9
- Ghisalberti, M., and Nepf, H. M. (2002). Mixing Layers and Coherent Structures in Vegetated Aquatic Flows. *J. Geophys. Res.* 107 (C2), 3011. doi: 10.1029/2001JC000871
- Ghisalberti, M., and Nepf, H. (2006). The Structure of the Shear Layer in Flows Over Rigid and Flexible Canopies. *Environ. Fluid. Mechanic.* 6 (3), 277–301. doi: 10.1007/s10652-006-0002-4
- Goldberg, W. M. (2018). *Coral Food, Feeding, Nutrition, and Secretion: A Review; in Marine Organisms as Model Systems in Biology and Medicine* Vol. Chap. 18. Eds. M. Kloc and J. Z. Kubiak (Gowerstrasse, Switzerland: Springer), 377–421, 2018.
- Hench, J. L., Leichter, J. J., and Monismith, S. G. (2008). Episodic Circulation and Exchange in a Wave-Driven Coral Reef and Lagoon System. *Limnol. Oceanogr.* 53, 2681–2694. doi: 10.4319/lo.2008.53.6.2681
- Hench, J. L., and Rosman, J. H. (2013). Observations of Spatial Flow Patterns at the Coral Colony Scale on a Shallow Reef Flat. *J. Geophys. Res. Ocean.* 118, 1142–1156. doi: 10.1002/jgrc.20105
- Jimenez, I. M., Kuhl, M., Larkum, A. W. D., and Ralph, P. J. (2011). Effects of Flow and Colony Morphology on the Thermal Boundary Layer of Corals. *J. R. Soc. Interface* 8, 1785–1795. doi: 10.1098/rsif.2011.0144
- Johnson, A., and Sebens, K. (1993). Consequences of a Flattened Morphology: Effects of Flow on Feeding Rates of the Scleractinian Coral *Meandrina Meandrites*. *Mar. Ecol. Prog. Ser.* 99 (1/2), :99–114.
- Jokiel, P. L. (1978). Effects of Water Motion on Reef Corals. *J. Exp. Mar. Biol. Ecol.* 35, 87–97. doi: 10.1016/0022-0981(78)90092-8
- Kaandorp, J. A., Lowe, C. P., Frenkel, D., and Sloot, P. M. A. (1996). Effect of Nutrient Diffusion and Flow on Coral Morphology. *Phys. Rev. Lett.* 77 (11), 2328. doi: 10.1103/PhysRevLett.77.2328
- Kaimal, J. C., and Finnigan, J. J. (1994). *Atmospheric Boundary Layer Flows Their Structure and Measurement* (New York: Oxford University Press).
- Kawaguti, S. (1954). Effects of Light and Ammonium on the Expansion of Polyps in Reef Corals. *Biol. J. Okayama Univ.* 2, 45–50.
- Koehl, M. A. R. (1999). Ecological Biomechanics of Benthic Organisms: Life History Mechanical Design and Temporal Patterns of Mechanical Stress. *J. Exp. Biol.* 202 (23), 3469–3476. doi: 10.1242/jeb.202.23.3469
- Levy, O., Dubinsky, Z., and Achituv, Y. (2003). Photobehavior of Stony Corals: Responses to Light Spectra and Intensity. *J. Exp. Biol.* 206, 4041–4049. doi: 10.1242/jeb.00622
- Levy, O., Dubinsky, Z., Achituv, Y., and Erez, J. (2006). Diurnal Polyp Expansion Behavior in Stony Corals may Enhance Carbon Availability for Symbionts Photosynthesis. *J. Exp. Mar. Biol. Ecol.* 333, 1–11. doi: 10.1016/j.jembe.2005.11.016
- Levy, O., Mizrahi, L., Chadwick-Furman, N. E., and Achituv, Y. (2001). Factors Controlling the Expansion Behavior of *Favia Favus* (Cnidaria: Scleractinia): Effects of Light, Flow, and Planktonic Prey. *Biol. Bull.* 200, 118–126. doi: 10.2307/1543305
- Lewis, J. B., and Price, W. S. (1975). Feeding Mechanisms and Feeding Strategies of Atlantic Reef Corals. *J. Zool.* 176, 527–544. doi: 10.1111/j.1469-7998.1975.tb03219.x
- Lowe, R. J., and Falter, J. L. (2015). Oceanic Forcing of Coral Reefs. *Annu. Rev. Mar. Sci.* 7, 43–66. doi: 10.1146/annurev-marine-010814-015834
- Lowe, R. J., Falter, J. L., Monismith, S. G., and Atkinson, M. J. (2009). Wave-Driven Circulation of a Coastal Reef-Lagoon System. *J. Phys. Oceanogr.* 39, 873–893. doi: 10.1175/2008JPO3958.1
- Lowe, R. J., Shavit, U., Falter, J. L., and Kosseff JR and Monismith, S. G. (2008). Modeling Flow in Coral Communities With and Without Waves: A Synthesis of Porous Media and Canopy Flow Approaches. *Limnol. Oceanogr.* 53 (6), 2668–2680. doi: 10.4319/lo.2008.53.6.2668
- Malul, D., Holzman, R., and Shavit, U. (2020). Coral Tentacle Elasticity Promotes an Out-of-Phase Motion That Improves Mass Transfer. *Proc. R. Soc. B.* 287, 20200180. doi: 10.1098/rspb.2020.0180
- Mass, T., Brickner, I., Hendy, E., and Genin, A. (2011). Enduring Physiological and Reproductive Benefits of Enhanced Flow for a Stony Coral. *Limnol. Oceanogr.* 56 (6), 2176–2188. doi: 10.4319/lo.2011.56.6.2176
- Mass, T., Genin, A., Shavit, U., Grinstein, M., and Tchernov, D. (2010). Flow Enhances Photosynthesis in Marine Benthic Autotrophs by Increasing the Efflux of Oxygen From the Organism to the Water. *Proc. Natl. Acad. Sci. (PNAS)* 107 (6), 2527–2531. doi: 10.1073/pnas.0912348107
- Mazzuoli, M., Blondeaux, P., Simeonov, J., and Calantoni, J. (2017). Direct Numerical Simulation of the Oscillatory Flow Around a Sphere Resting on a Rough Bottom. *J. Fluid. Mechanic* 822, 235–266. doi: 10.1017/jfm.2017.242
- Moltchanov, S., Bohbot-Raviv, Y., Duman, T., and Shavit, U. (2015). Canopy Edge Flow: A Momentum Balance Analysis. *Water Resour. Res.* 51 (4), 2081–2095. doi: 10.1002/2014WR015397
- Monismith, S. G. (2007). Hydrodynamics of Coral Reefs. *Annu. Rev. Fluid. Mechanic* 39 (1), 37–55. doi: 10.1146/annurev.fluid.38.050304.092125
- Nakamura, T., van Woesik, R., and Yamasaki, H. (2005). Photoinhibition of Photosynthesis is Reduced by Water Flow in the Reef-Building Coral *Acropora Digitifera*. *Mar. Ecol. Prog. Ser.* 301, 109–118. doi: 10.3354/meps301109
- Nepf, H. M. (2012). Flow and Transport in Regions With Aquatic Vegetation. *Annu. Rev. Fluid. Mechanic* 44, 123–142. doi: 10.1146/annurev-fluid-120710-101048
- Park, S., Piriatskiy, G., Zeevi, D., Ben-David, J., Yossifon, G., Shavit, U., et al. (2017). The Nematocyst's Sting is Driven by the Tubule Moving Front. *J. R. Soc. Interface* 14 (128), 2017. doi: 10.1098/rsif.2016.0917
- Patterson, M. R. (1991). The Effects of Flow on Polyp-Level Prey Capture in an Octocoral. *Alcy. Siderium. Biol. Bull.* 180, 93–102. doi: 10.2307/1542432
- Patterson, M. R. (1992). A Mass-Transfer Explanation of Metabolic Scaling Relations in Some Aquatic Invertebrates and Algae. *Science* 255, 1421–1423. doi: 10.1126/science.255.5050.1421
- Patterson, M. R., and Sebens, K. P. (1989). Forced Convection Modulates Gas Exchange in Cnidarians. *Proc. Natl. Acad. Sci. (PNAS)* 86, 8833–8836. doi: 10.1073/pnas.86.22.8833
- Porter, J. (1974). Zooplankton Feeding by the Caribbean Reef-Building Coral *Montastraea Cavernosa*. *Proc. 2nd. Int. Coral. Reef. Symp.* 1, 111–125.
- Ramponi, R., Blocken, B., de Co, L. B., and Janssen, W. D. (2015). CFD Simulation of Outdoor Ventilation of Generic Urban Configurations With Different Urban Densities and Equal and Unequal Street Widths. *Build. Environ.* 92, 152–166. doi: 10.1016/j.buildenv.2015.04.018
- Reidenbach, M. A., Stocking, J. B., Szczyrba, L., and Wendelken, C. (2021). Hydrodynamic Interactions With Coral Topography and Its Impact on Larval Settlement. *Coral. Reef.* 40, 505–519. doi: 10.1007/s00338-021-02069-y
- Rosman, J. H., and Hench, J. L. (2011). A Framework for Understanding Drag Parameterizations for Coral Reefs. *J. Geophys. Res. Ocean* 116, 1–15. doi: 10.1029/2010JC006892

- Rosman, J. H., Koseff, J. R., Monismith, S. G., and Grover, J. (2007). A Field Investigation Into the Effects of a Kelp Forest (*Macrocystis Pyrifera*) on Coastal Hydrodynamics and Transport. *J. Geophys. Res.-Ocean.* 112, C02016. doi: 10.1029/2005JC003430
- Sebens, K. P., Grace, S. P., Helmuth, B., Maney, E. J., and Miles, J. S. (1998). Water Flow and Prey Capture by Three Scleractinian Corals. *Madracis Mirabilis*, *Montastrea Cavernosa* and *Porites Porites*, in a Field Enclosure. *Mar. Biol.* 131, 347–360. doi: 10.1007/s002270050328
- Sebens, K. P., and Johnson, A. S. (1991). Effects of Water Motion on Prey Capture and Distribution of Reef Corals. *Hydrobiologia* 226, 91–101. doi: 10.1007/BF00006810
- Shapiro, O. H., Fernandez, V. I., Garren, M., Guasto, J. S., Debaillon-Vesque, F. P., Kramarsky-Winter, E., et al. (2014). Vortical Ciliary Flows Actively Enhance Mass Transport in Reef Corals. *Proc. Natl. Acad. Sci. (PNAS)* 111 (37), 13391–13396. doi: 10.1073/pnas.1323094111
- Shashar, N., Cohen, Y., and Loya, Y. (1993). Extreme Diel Fluctuations of Oxygen in Diffusive Boundary Layers Surrounding Stony Corals. *Biol. Bull.* 185, 455–461. doi: 10.2307/1542485
- Shavit, U., Lowe, R. J., and Steinbuck, J. V. (2007). Intensity Capping: A Simple Method to Improve Cross-Correlation PIV Results. *Exp. Fluid.* 42 (2), 225–240. doi: 10.1007/s00348-006-0233-7
- Sheppard, C. R. C., Davy, S. K., Pilling, G. M., and Graham, N. A. J. (2018). *The Biology of Coral Reefs, 2nd Ed* (University Press, Oxford: Oxford).
- Sorokin, Y. U. I. (1990). “Plankton in the Reef Ecosystems,” in *Ecosystems of the World: Coral Reefs*. Ed. Z. Dubinsky (Amsterdam: Elsevier), 291–327.
- Stocking, J. B., Laforsch, C., Sigl, R., and Reidenbach, M. A. (2018). The Role of Turbulent Hydrodynamics and Surface Morphology on Heat and Mass Transfer in Corals. *J. R. Soc Interface* 15, 20180448. doi: 10.1098/rsif.2018.0448
- Sveen, J. (2004). *An Introduction to MatPIV V 1.6.1 Mechanics and Applied Mathematics* (Norway: Department of Mathematics. University of Oslo).
- Sweeney, B. (1976). Circadian Rhythm in Corals, Particularly Fungiidae. *Biol. Bull.* 151, 236–246. doi: 10.2307/1540717
- Thomas, F. I. M., and Atkinson, M. J. (1997). Ammonium Uptake by Coral Reefs: Effects of Water Velocity and Surface Roughness on Mass Transfer. *Limnol. Oceanogr.* 42, 81–88. doi: 10.4319/lo.1997.42.1.0081
- Todd, P. A. (2008). Morphological Plasticity in Scleractinian Corals. *Biol. Rev.* 83, 315–337. doi: 10.1111/j.1469-185X.2008.00045.x
- van Woesik, R., Irikawa, A., Anzai, R., and Nakamura, T. (2012). Effects of Coral Colony Morphologies on Mass Transfer and Susceptibility to Thermal Stress. *Coral. Reef* 31, 633–639. doi: 10.1007/s00338-012-0911-2
- Yosef, O., Popovits, Y., Malik, A., Ofek-Lalzer, M., Mass, T., and Sher, D. (2020). A Tentacle for Every Occasion: Comparing the Hunting Tentacles and Sweeper Tentacles, Used for Territorial Competition, in the Coral *Galaxea Fascicularis*. *BMC Genomics* 21, 548. doi: 10.1186/s12864-020-06952-w
- Yu, X., Rosman, J. H., and Hench, J. L. (2022). Boundary Layer Dynamics and Bottom Friction in Combined Wave-Current Flows Over Large Roughness Elements. *J. Fluid. Mech.* 931, A11–1–29. doi: 10.1017/jfm.2021.941

Conflict of Interest: The authors declare that the research was conducted in the absence of any commercial or financial relationships that could be construed as a potential conflict of interest.

Publisher’s Note: All claims expressed in this article are solely those of the authors and do not necessarily represent those of their affiliated organizations, or those of the publisher, the editors and the reviewers. Any product that may be evaluated in this article, or claim that may be made by its manufacturer, is not guaranteed or endorsed by the publisher.

Copyright © 2022 Shavit, Mass and Genin. This is an open-access article distributed under the terms of the Creative Commons Attribution License (CC BY). The use, distribution or reproduction in other forums is permitted, provided the original author(s) and the copyright owner(s) are credited and that the original publication in this journal is cited, in accordance with accepted academic practice. No use, distribution or reproduction is permitted which does not comply with these terms.